Communications and Networking

Academic and research staff
Professor Vincent W. S. Chan

Visiting scientists and research affiliates
John Chapin (VANU Inc.), Professor Guevara Noubir (Northeastern University), Professor Ashwin Gumaste (IIT, Mumbai), Steven Finn, Alan Kirby (CISCO), Terrence MacGarty, Eric Swanson, Lillian Dai, Guy Weichenberg

Postdoctoral Fellow
Ingrid Lin

Graduate students
Anurupa Ganguly, James Glettler, Etty Lee, Andrew Puryear, Guy Weichenberg, Zhang Lei

Undergraduate student
Mia Yinuo Qian

Technical and support staff
Susanne Patterson, Elizabeth Reid

Overview of the research in the Communication and Network Group
Research in the group includes topics on networks and communication systems. The work extends to applications in satellite, wireless and optical communication, and data networks. The objective is to develop the scientific base needed to design data communication networks that are efficient, robust and architecturally clean. Wide-area and local-area networks, high-speed networks, and point-to-point and broadcast communication channels are of concern. Topics of current interest include network architectures at all network layers; power control; multiple antenna techniques; media access control protocols; routing in optical, wireless and satellite networks; quality of service control; failure recovery; topological design; and the use of efficient resource allocation for network connectivity and QoS. An important new research frontier that will call for new modeling, analysis and architecture optimization is the next frontier of networks over fiber systems with agile and economical service delivery and fast, dynamically changing communication media, such as mobile wireless communication in the presence of fast fading and changing connectivities, microwave satellite communication and free space optical communication over rapidly changing atmospheric phenomena and dealing with unscheduled, bursty, large-granularity users at the edge of networks. The problems in this direction are important, rich and very challenging. The research usually requires multi-disciplinary techniques and tools to tackle.

A major new theme of the group is the pursuit of research that cuts across multiple communications modalities; optical, wireless and satellite networks. The theme of heterogeneous networking with performance guarantees is a challenging and important problem for defense and high-end commercial applications. A significant component of our research is the creation of new architectures guided by the understanding of technology and fundamental system limits and the realization and validation of these architectures with hardware and algorithms and system demonstrations. As such, we work closely with industry to extend our research reach and impact beyond the academic boundary.

1 Future Optical Network Architecture

Sponsors
DARPA – FONA: HR0011-08-1-0008
National Science Foundation (NSF) – FIND:CNS-0626800 and GOALI: CNS-0831612

Project Staff and other Participants
Vincent W. S. Chan, Anurupa Ganguly, Ori Gerstel (Cisco Systems), Kyle Guan, Ashwin Gumaste (Indian Institute of Technology), Eric Swanson, Guy Weichenberg, Zhang Lei, Ingrid Lin, Dan Kilper (Alcatel Lucent Bell Labs.)

Optical networking has enabled the Internet as we know it today, and is central to the realization of Network-Centric Warfare in the defense world. Sustained exponential growth in communications bandwidth demand, however, is requiring that the nexus of innovation in optical networking continue, in order to ensure cost-effective communications in the future.

In our work, we developed the concept of Optical Flow Switching (OFS) and showed it to be a key enabler of scalable future optical networks. The general idea behind OFS – agile, end-to-end, all-optical connections – is several years old. However, owing to the absence of an application for it, OFS remained under-developed – bereft of how it could be implemented, how well it would perform, and how much it would cost relative to other architectures. Our contributions are in providing partial answers to these three broad questions. With respect to implementation, we addressed the physical layer design of OFS in the metro-area and access, and developed sensible scheduling algorithms for OFS communication. Our performance study comprised a comparative capacity analysis for the wide-area, as well as an analytical approximation of the throughput-delay tradeoff offered by OFS for inter-MAN communication. Lastly, with regard to the economics of OFS, we employed an approximate capital expenditure model, which enabled a throughput-cost comparison of OFS with other prominent candidate architectures. Our conclusions point to the fact that OFS indeed offers significant advantage over other architectures in economic scalability. In particular, for sufficiently heavy traffic, OFS handles large transactions at far lower cost than other optical network architectures. In light of the increasing importance of large transactions in both commercial and defense networks, we conclude that OFS may be crucial to the future viability of optical networking.

1.1 Physical Architecture

Our recent research on Optical Flow Switching (OFS) has provided partial answers as to how the architecture could be implemented, how well it would perform, and how much it would cost relative to other architectures. Owing to the absence of buffering and optical-electronic-optical (OEO) conversions in the interior of OFS networks, the economic viability of OFS hinges, in large part, on cost-effective deployment of all-optical networking components in the metro-area and access to carry out optical aggregation of data – while, of course, respecting the stringent physical layer constraints imposed by the architecture. In metro-area networks (MANs), reconfigurability via (expensive) optical cross-connects (OXCs) is economically justifiable, owing to the large number of end-users supported; whereas (less expensive) broadcast architectures, coupled with reservation/scheduling, are appropriate for access networks, where the number of supported end-users is significantly smaller. Given these assumptions, we derived high-level physical layer constraints for both inter- and intra-MAN OFS communication. For the metro-area, we specialized our results to mesh networks based upon Generalized Moore Graphs (to be justified with a cost analysis in section 3) with optical amplifiers compensating for OXC losses. In the access environment, conventional passive optical network (PON) designs are inadequate for OFS distribution networks, owing to the more stringent physical layer constraints arising from the absence of OEO conversion at the head-end. As a result, we proposed and analyzed a family of all-optical distribution networks that employ multiple Erbium-doped fiber (EDF) segments *within* the network (see Figure 1-1), in contrast to conventional PON schemes which employ a single, lumped amplifier at the head-end. Our proposed design results in better signal quality – as summarized in the figure – allowing for the realization of OFS. Moreover,

such designs can be made economically viable by employing a remotely-pumped configuration – as indicated in the figure – in which a single laser supplies power to all of the EDF segments.

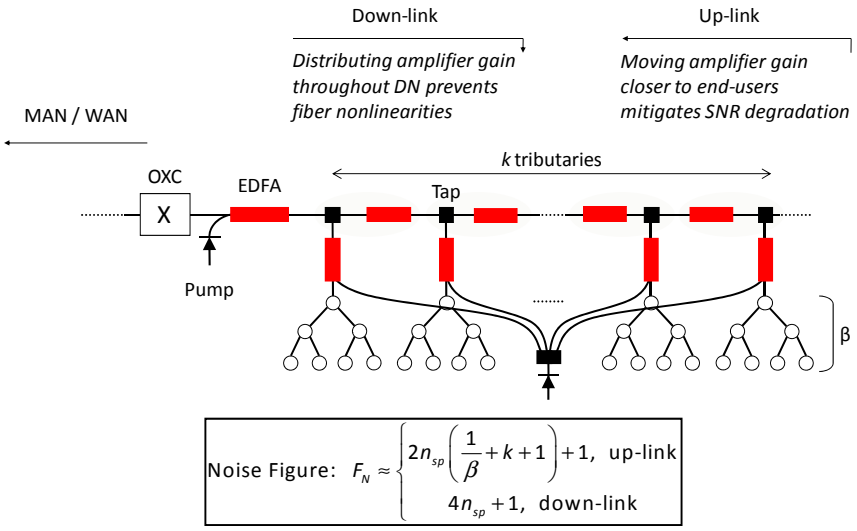

Figure 1-1: Internally amplified distribution network design with two alternative remote pumping schemes.

1.2 Performance

In our previous work, we carried out a comparative network capacity analysis of OFS with other optical network architectures [Weichenberg07]. Our more recent work has addressed the throughput-delay tradeoff for inter-MAN OFS communication.

In the wide-area, we assumed a quasi-static logical topology – that is, wavelength channels are reconfigured on time-scales that are much longer than that of individual transactions – owing to statistical multiplexing of a large number of transactions. This assumption permits decoupling of scheduling in the wide-area on short time-scales among MAN pairs. To ensure manageable algorithmic complexity in the metro-area an access: i) we augment links carrying inter-MAN traffic with additional capacity, and ii) employ a simple, sequential scheduling algorithm which reserves resources in the MAN and wide-area network (WAN) first, followed by reservation of resources in the access.

Figures 1.2-1 and 1.2-2 illustrate our analytic approximations of the throughput-delay tradeoff under our assumptions. In Figure 2-1, the tradeoff is depicted for different transaction length distributions. In Figure 2-2, the tradeoff is illustrated for MANs with a fixed amount of (heavy-tailed) traffic, but with a different number of distribution networks over which to spread this traffic. It is observed that, for large MANs (i.e., large number of distribution networks), the throughput-delay tradeoff is close that of an optimal scheduling algorithm (with unmanageable complexity). This is because under such circumstances, the existence of little contention for network resources within the distribution networks enables our algorithm performs almost optimally. This suggests that there is a minimum-cost number of distribution networks to serve a given traffic demand. We carried out this optimization as part of our throughput cost study, as discussed next.

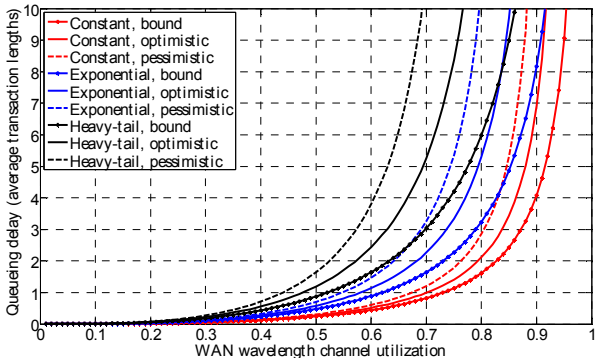

Figure 1.2-1: Throughput-delay tradeoff for different transaction length distributions.

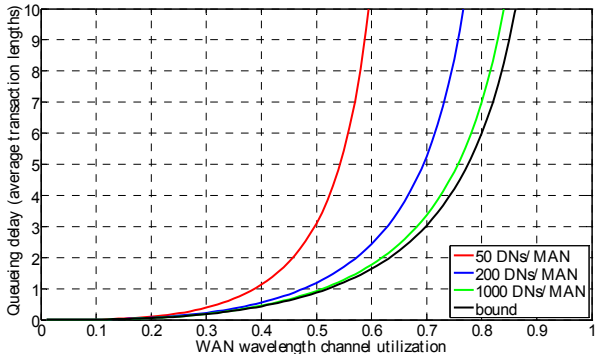

Figure 1.2-2: Throughput-delay tradeoff for different numbers of distribution networks per MAN, assuming heavy-tailed traffic.

1.3 Throughput-cost comparison of architectures

Previously, we carried out a simple throughput-cost comparison of OFS with other optical network architectures [Weichenberg06]. We recently refined our analysis in the following two ways: i) we formulated a more comprehensive cost model, employing additional source of capital expenditure (CapEx); ii) we optimized the physical layers of the architectures that we compared, in order to obtain a "best-case" scenario for each architecture. Our major conclusion is: *OFS is the most cost-scalable architecture of all, in that its asymptotic normalized cost is several times lower than that of competing architectures.*

The two traditional optical network architectures that we compared OFS to are electronic packet switching (EPS) and optical circuit switching (OCS/EPS). EPS networks employ fiber for transport between nodes in the MAN and WAN, and electronic aggregation, routing, and switching at nodes. In the access, PONs with OEO conversions at the head-end are employed. We define OCS/EPS to be identical to EPS in the access and MAN, but employing optical circuits between WAN edge routers with optical bypass via OXCs at intermediate nodes. In our study, we also investigated the throughput-cost tradeoffs offered by hybrid architectures – architectures comprising two or more of the aforementioned homogeneous network architectures. We point out that the EPS-OCS/EPS hybrid architecture resembles the Generalized Multiprotocol Label Switching (GMPLS) architecture.

In our throughput-cost study, we assumed that all of the architectures considered operate on the same WAN fiber plant topology: a 60 node network introduced in [Simmons08] as a representative US carrier backbone network. The sets of WAN node pair traffic demands that we consider are uniformly scaled versions of the set employed in [Simmons08]. This traffic set reflects actual US backbone network traffic, and is therefore not uniform all-to-all in nature.

In the metro-area, we analytically optimized the fiber topology in accordance with the switching and fiber deployment costs particular to each architecture. We restricted our consideration of fiber plant topologies to those that are based upon regular graphs with nodal symmetry, since such topologies are reasonable models of real MANs and are more analytically tractable. With respect to traffic in the MAN, we assumed that intra-MAN traffic is uniform all-to-all, whereas inter-MAN traffic is uniform all-to-one (and one-to-all) to (from) the gateway node of the MAN. We found that the family of Generalized Moore Graphs minimizes cost, albeit with different dimensions for different architectures. Under the assumption that switching cost is linear with the number of ports, we analytically solved for the optimal node degree which balances switching and fiber cost (see Figure 1.3-1).

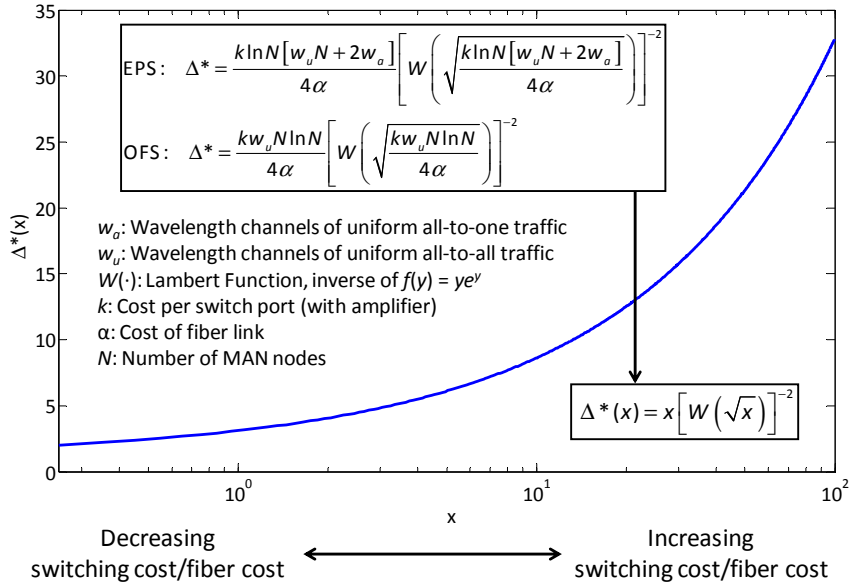

Figure 1.3-1: Optimal MAN node degree Δ* which balances switching and fiber cost. A switch cost that scales linearly with the number of ports is assumed.

In the access, we employed distribution networks with remotely pumped EDFs (discussed in section 1), which support a large number of end-users economically. Our design for EPS and OCS/EPS employs an optical line terminal (OLT) at the head-end, whereas our OFS distribution network connects to the MAN passively and transparently. With respect to individual end-user data rate requirements, we considered both homogeneous and heterogeneous requirements.

Our cost model focused on CapEx and neglected ongoing operating expenditure (OpEx). The CapEx cost components included are: fiber, switching/routing, amplification, dispersion compensation, regeneration, and transceivers. We accounted for cost differences arising from varying optical reach and line-rate. We assumed 40 Gbps line-rate throughout, except for distribution networks in EPS and OCS/EPS, for which a 10 Gbps line-rate was assumed.

1.4 Homogeneous architectures

In Figure 1.3-2, we indicate the minimum-cost architecture as a function of number of end-users per MAN and average end-user data rate; and in Figure 1.3-3, we depict a horizontal cross-section of Figure 1.3-2 at a MAN population of 10^6 end-users. When aggregate traffic is low, EPS is seen to be the most sensible architecture. Electronic switches and routers, to be sure, are less economically scalable technologies than OXCs, but they operate at finer data granularities than OXC. Thus, when aggregate traffic is low, it is wasteful to provision entire wavelength-granular OXC ports that are poorly utilized – which is why EPS is the minimum-cost architecture in this regime of operation. However, when traffic increases, optical switching in the WAN is sensible, rendering OCS/EPS the minimum-cost architecture. As aggregate traffic grows even larger, optical switching in the MAN and at the access boundary is most economical, rendering OFS the minimum-cost architecture.

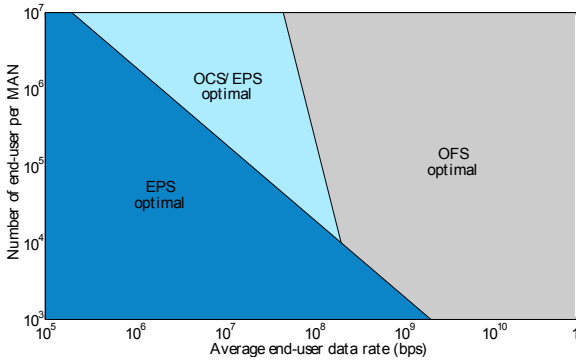

Figure 1.3-2: Minimum-cost homogeneous architecture as a function of MAN size and average end-user data rate

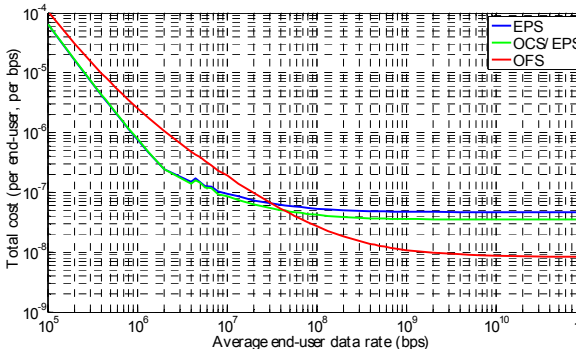

Figure 1.3-3: Normalized network cost vs. average end-user data rate. Each MAN has 10^6 end-users.

1.5 Hybrid architectures

In Figure 1.3-4, we indicate the minimum-cost hybrid architecture as a function of the number of end-users per MAN and average end-user data rate. As in Figure 3-2, when aggregate traffic is relatively low, the homogeneous EPS architecture is optimal for the reasons discussed above. However, as aggregate traffic increases, we found that hybrid architectures become preferable to homogeneous architectures. Specifically, we found that with increasing traffic, OCS/EPS, and subsequently OFS, become components of the minimum-cost hybrid architecture. In Figure 3-5, we depict a horizontal cross-section of the minimum-cost hybrid architecture in Figure 3-4 at a MAN population of 10^6 end-users. The black curve, which represents the normalized cost of the entire hybrid architecture, is essentially a weighted average of the three colored subarchitecture curves. At low average end-user data rates the (black) hybrid architecture curve follows the (blue) EPS curve, and for high average end-user data rates the hybrid architecture curve follows the (red) OFS curve, indicating the dominance of these architectures at these two extremes.

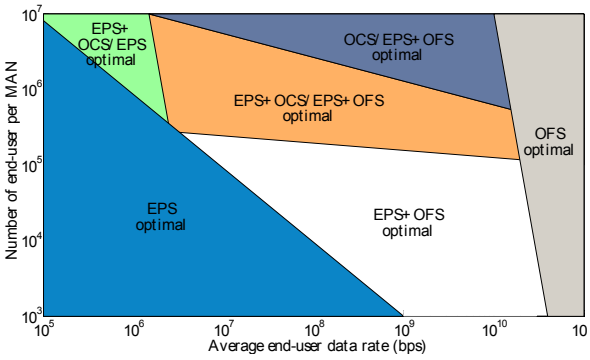

Figure 1.3-4: Minimum-cost hybrid architecture as a function of MAN size and end-user average data rate

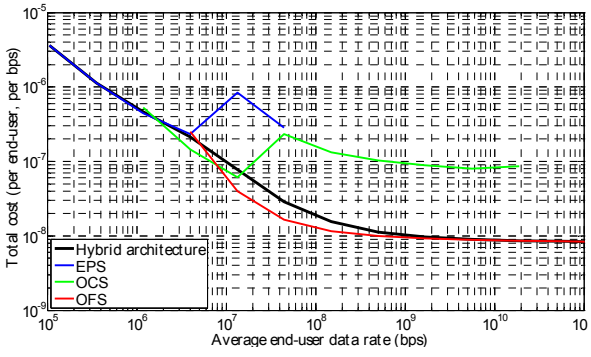

Figure 1.3-5: Normalized cost components of minimum-cost hybrid architecture / fraction of traffic vs. average end-user data rate. Each MAN has 10^6 end-users.

In sum, we found that, for large average end-user data rates, OFS is the most economically attractive homogeneous architecture and a critical component of hybrid architectures owing to an asymptotic normalized cost several times lower than that of competing architectures.

References

[Simmons08] J. Simmons, *Optical Network Design and Planning*, (Springer, 2008), Chapter 8.

[Weichenberg06] G. Weichenberg, V.W.S. Chan, and M. Médard, “On the throughput-cost tradeoff of optical network architectures,” IEEE Globecom, 2006.

[Weichenberg07] G. Weichenberg, V.W.S. Chan, and M. Médard, “On the capacity of optical networks: A framework for comparing different transport architectures,” IEEE JSAC-OCN, 2007.

2 Coherent Optical Communication and Network

Sponsors
DARPA –TACOTA: W91NF-06-1-0062
ONR- Free space optical heterodyne communication and network: N00014-09-1-0131

Project Staff
Vincent W. S. Chan, Andrew Puryear, James Glettler.

Our research addressed the feasibility of an optical wireless network over the atmosphere in the presence of turbulence and interference, Figure 2.1. These networks will have significant impact for over land and ocean applications as well as links to aircraft and satellites. Data rates of over 100 Gbps can be supported but only with the right mitigation techniques against various impediments. The big challenge is to engineer the free space optical wireless communication in the presence of atmospheric turbulence/weather and intentional interference so network protocols can run over these links.

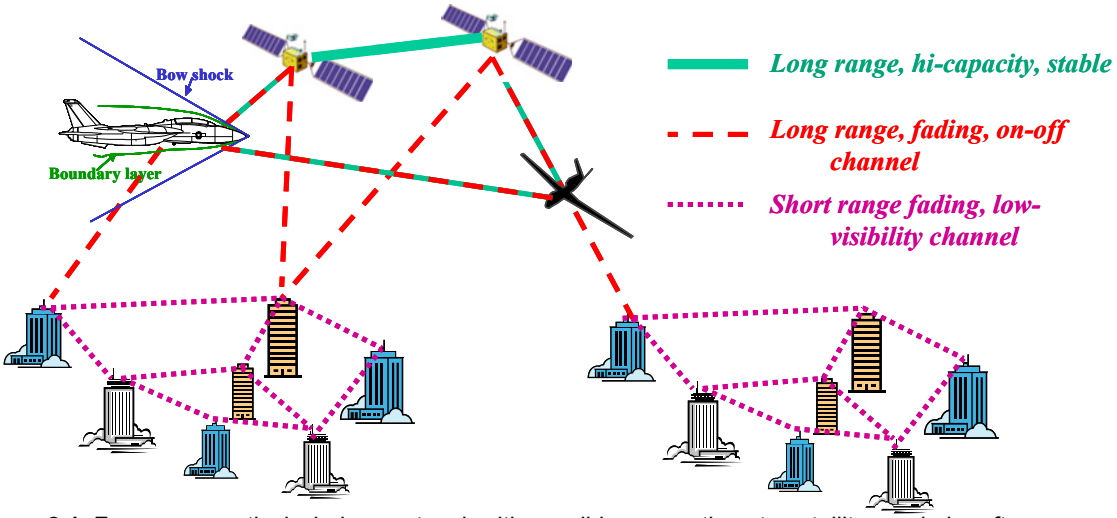

Figure 2.1. Free space optical wireless network with possible connections to satellites and aircraft.

The program was conducted with the following two goals:

> *1. Demonstrate the superiority of diversity coherent systems over direct detection systems in the mitigation of fading due to atmospheric turbulence and background noise rejection.*
>
> *2. Demonstrate the superior performance of coherent systems against jamming including using near-field transmitter and receiver phase and amplitude control with feedback*

2.2 Diversity Systems

Diversity is a sensible technique to mitigate fading experienced in free space optical communication because of the improvement in average fading statistics that it provides. Moreover, in the presence of background noise and an intelligent interferer, diversity *coherent* detection is preferable over diversity *direct* detection. This is due to coherent detection's ability to limit the amount of unwanted background noise and interference detected.

Using a log-normal fading model for the clear atmospheric channel, we derived the outage probability of diversity incoherent and coherent systems in the absence of and presence of an intelligent interferer that may take on various transmission strategies. The interferer strategy that causes the most damage for high error probability thresholds in direct detection is one that tries to mask the signal with Gaussian noise, and in coherent detection is one that cancels the signal. In direct

detection, increasing diversity beyond a threshold value actually begins to degrade performance because, as diversity increases, the amount of interference and background noise detected increases. This optimal diversity degree for direct detection occurs when the improvement in fading statistics from diversity is counterbalanced by the added background noise and /or detected interference signal. We derived this optimal diversity degree both in the absence of and presence of interference. In coherent detection, increasing diversity always improves performance.

In order to compare diversity coherent detection with diversity direct detection from many perspectives, we analyzed the power gain of diversity coherent detection over diversity direct detection in the presence of and absence of an interferer, and where direct detection's diversity is fixed to its optimal value and where it varies. Diversity coherent detection provides significantly better performance over diversity direct detection receivers and most of this performance gain can be achieved with a moderate amount of diversity.

In contrast to spatial diversity for wireless systems, spatial diversity for atmospheric optical systems can be readily implemented in a compact fashion, since the coherence length is of the order of centimeters. i. e. multiple transmitters or receivers only need to be placed centimeters apart to see approximately independent channel fades. It is possible to dynamically configure the array transmitters and array receivers at the nodes of a coherent optical wireless network to provide substantial performance gains, Figure 2.2.

2.3 Transmitter and receiver arrays

The available diversity equals the product of the number of independent (in the sense of being in different phase coherence cells) transmitter elements and receiver elements. If a low rate (~10kbps) feedback link is available between the receiver and the transmitter, there is the possibility of transmitter phase pre-distortion to help focus the optical energy on the receiver array, enhancing energy delivery efficiency of the free space channel. Receiver phase tracking element by element either via local-oscillator (LO) tuning or signal path phase modulation will be demonstrated in this program and the data fed back to the transmitter for phase and amplitude modulation of the individual array elements.

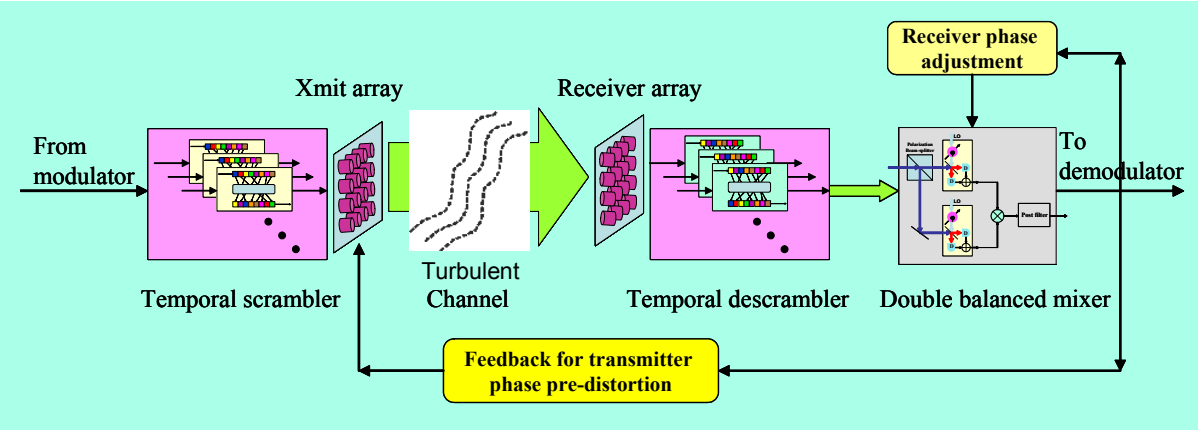

Figure 2.2. Transmission system with dynamically and adaptively reconfigurable receiving plane field patterning, crypto-key driven frequency spreading and time interleaving.

2.4 Performance gains of coherent systems in the presence of turbulence, background noise, and jamming

When communicating optically through the clear atmospheric channel, not only is there atmospheric turbulence and background noise, but an intentional interferer may also be present. Even if the interferer is off-axis, its signal can couple into the receiver through scattering. We would like our communication system to perform well despite the presence of an interferer, background noise and fading. Figures 3 and 4 show block diagrams of the diversity direct detection and diversity coherent detection systems we considered for mitigating the unwanted signals and fading.

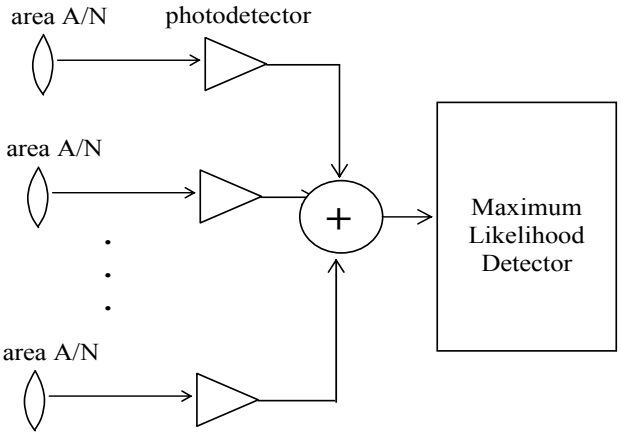

Figure 2.3. Block Diagram of multi-aperture (diversity N) diffraction limited direct detection, modulation scheme BPPM

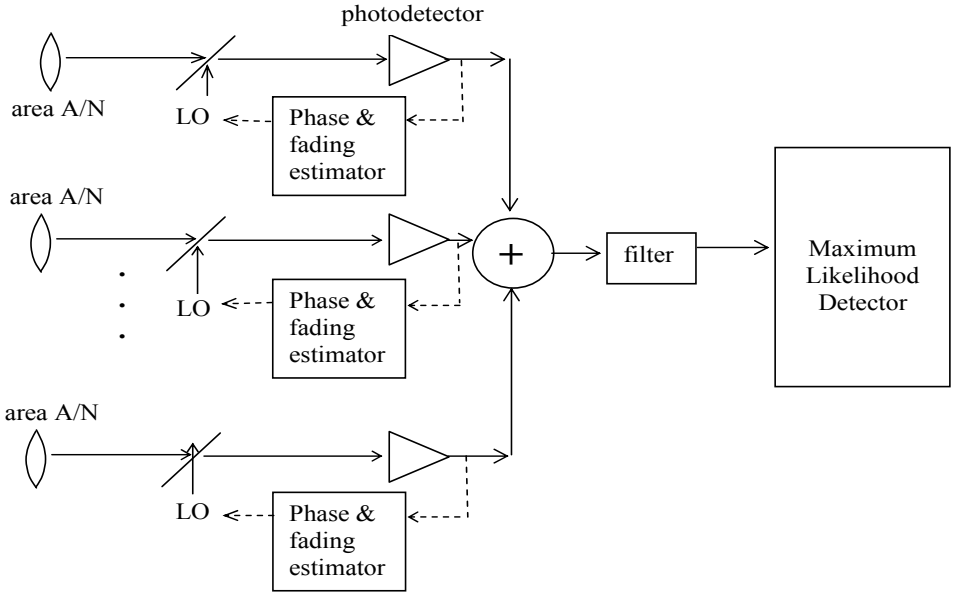

Figure 2.4. Block Diagram of multi-aperture (diversity N) coherent detection, modulation scheme BPSK

In the absence of any interferer, diversity direct detection's and diversity homodyne detection's outage probability are given by

$$P_{outage,DD,noInterference} = Q\left(\frac{m_U - \ln\left(\frac{1}{N_S}\left[\theta_{thresh} + \sqrt{2\theta_{thresh}NN_n}\right]\right)}{\sigma_U}\right) \approx \frac{1}{2}\exp\left\{-\frac{1}{2\sigma_U^2}\left[m_U - \ln\left(\frac{\left[\theta_{thresh} + \sqrt{2\theta_{thresh}NN_n}\right]}{N_S}\right)\right]^2\right\}$$

and

$$P_{outage,Homo,noInterference} = Q\left(\frac{m_U - \ln\left(\frac{(1+N_n)(-\ln 2 + \theta_{thresh})}{2N_s}\right)}{\sigma_U}\right) \approx \frac{1}{2}\exp\left\{-\frac{1}{2\sigma_U^2}\left[m_U - \ln\left(\frac{(1+N_n)(-\ln 2 + \theta_{thresh})}{2N_s}\right)\right]^2\right\}$$

respectively where N_n represents the average number of received background noise photons per symbol per receiver, and N_s represents the total average number of received signal photons per symbol, θ_{thresh} is the threshold error exponent below which an outage occurs, m_U and σ_U are the mean and standard deviation of the log of the average of the N power fading factors, and Q( ) is the Q-function.

Figure 2.5 plots the outage probability of the direct detection and homodyne detection systems in the absence any interferer. or direct detection, increasing diversity improves the outage probability initially, but then begins to degrade it. This is because diversity improves the fading statistics but also adds more background noise. We derive the optimal direct detection diversity value, N_{opt}, (the value at which the improvement in outage statistics from diversity begins to be overpowered by the added background noise) to be the root (that is ≥1) of the following equation

$$0 = a_3 N_{opt}^{3/2} + a_2 N_{opt} + a_1 N_{opt}^{1/2} + a_0$$

Where

$$a_3 = \sqrt{2N_n}$$

$$a_2 = -2\sqrt{-N_n\left(e^{4\sigma_\chi^2} - 1\right)\ln\left(2P_{outage}\right)}$$

$$a_1 = -\sqrt{-\theta^{thresh}\left(e^{4\sigma_\chi^2} - 1\right)\ln\left(2P_{outage}\right)}$$

$$a_0 = -\sqrt{\frac{\theta^{thresh}}{2}}\left(e^{4\sigma_\chi^2} - 1\right)$$

and where we assumed $\frac{e^{4\sigma_\chi^2} - 1}{N} << 1$. σ_χ^2 represents the variance of the log of each amplitude fading factor, and P_{outage} is the outage probability. For homodyne detection, increasing diversity always improves the outage probability because the fading statistics improve while the amount of background noise stays the same. In fact, for large diversity, the improvement in outage probability with diversity goes as

$$P_{outage,\,Homo,noInterference} \sim \frac{1}{2}\exp\{-cN\}$$

where $c = \frac{\left[\ln\left(\frac{(1+N_n)(-\ln 2 + \theta_{thresh})}{2N_S}\right)\right]^2}{2\left(e^{4\sigma_\chi^2} - 1\right)}$.

Note from Figure 2.5 for any given diversity *N*, homodyne detection has lower outage probability than direct detection.

We also consider the performance of our diversity communication systems in the presence of various types of intelligent interferers. Interference can couple into the receiver as in Figure 6. The interferer can cause the most damage if it optimizes its duty cycle. Tables 2.1 and 2.2 list the worse case duty cycle and the corresponding error probability and outage probability for the various interferer types. N_I represents the average received interferer photons detected per symbol per receiver.

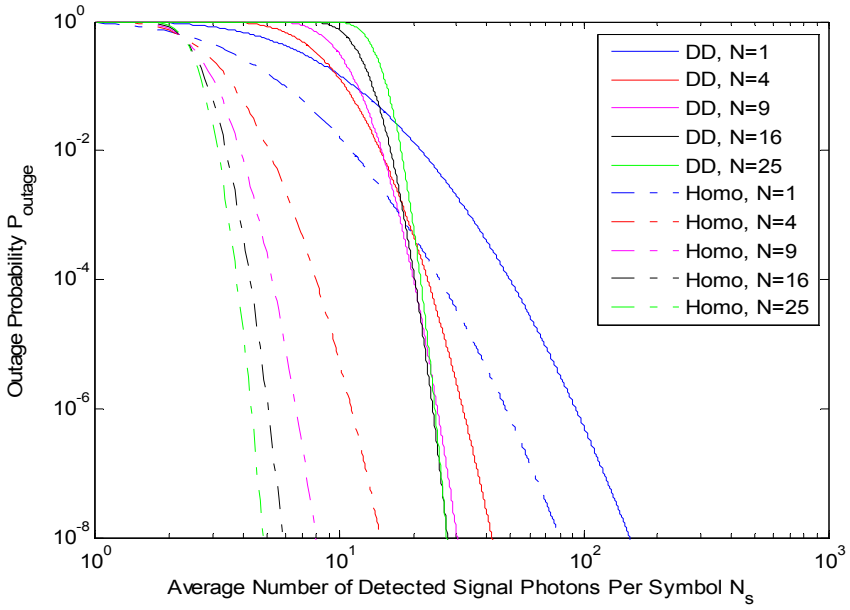

Figure 2.5. Outage probability in the absence of interference when P_e^{thresh} =0.1, σ_χ =0.3, N_n=1

For direct detection, notice that for all the interference types, the duty cycle, error probability, and outage probability increase linearly with increasing diversity. Since more interference is detected per symbol as diversity increases, the interferer can thus increase its duty cycle to cause more damage to more symbols. This causes the corresponding error probability and outage probability to increase. Direct detection's outage probability worsens with diversity because although the fading statistics improve with diversity, the total interference and background noise detected increases with diversity and overpowers the improvement in fading statistics. In fact, we proved that in the presence of the worst interferer considered (Gaussian interferer that transmits for the first half symbol), when the error probability threshold is high, the optimal diversity for direct detection is $N_{optGaussianHalfSymbolInterference}$=1. In other words, the lowest outage probably is achieved in direct detection if no diversity is used.

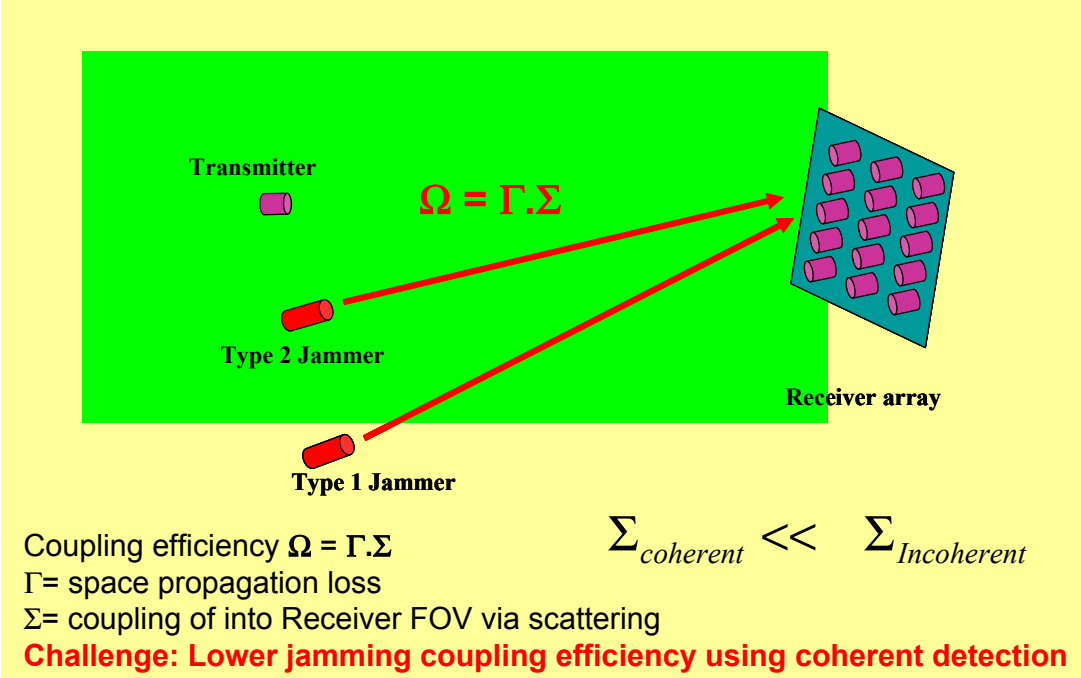

Figure 2.6. Background noise and interference coupling into receiver array.

For coherent detection however, increasing diversity does not cause an increase in duty cycle, error probability or outage probability because. Homodyne detection's outage probability improves with diversity because the fading statistics improve while the total amount of detected interference remains the same.

Interferer type	Worst case duty cycle in absence of turbulence	Worst case duty cycle in presence of turbulence
Direct Detection:		
Constant on for entire symbol	$\frac{2NN_I}{N_S^2}$	$\frac{2NN_I\theta_{thresh}}{N_S^2}\left(1+\frac{e^{4\sigma_\chi^2}-1}{N}\right)^5$
Constant on for half symbol	$\frac{NN_I}{N_S}$	$\frac{NN_I}{N_S}\left(1+\frac{e^{4\sigma_\chi^2}-1}{N}\right)^{3/2}$
Gaussian on for entire symbol	$\frac{NN_I}{N_S}$	$\frac{NN_I}{N_S}\sqrt{2(-\ln 2+\theta_{thresh})}\left(1+\frac{e^{4\sigma_\chi^2}-1}{N}\right)^{3/2}$
Gaussian on for half symbol	$\frac{2NN_I}{N_S}$	$\frac{NN_I}{N_S}\left(2\sqrt{-\ln 2+\theta_{thresh}}+1\right)\left(1+\frac{e^{4\sigma_\chi^2}-1}{N}\right)^{3/2}$
Canceling on for entire symbol	$\frac{2NN_I}{N_S}$	$\frac{2NN_I}{N_S}$
Canceling on for half symbol	$\frac{NN_I}{N_S}$	$\frac{NN_I}{N_S}$
Homodyne Detection:		
Gaussian	$\frac{N_I}{2N_S}$	$\frac{N_I}{2N_S}(-\ln 2+\theta_{thresh})\left(1+\frac{e^{4\sigma_\chi^2}-1}{N}\right)^{3/2}$
Canceling	$\frac{N_I}{N_S}$	$\frac{N_I}{N_S}\left(1+\frac{e^{4\sigma_\chi^2}-1}{N}\right)^{3/2}$

Table 2.1. Worst case interferer duty cycle for various interferer types

Interferer type	Error probability (in absence of turbulence)	Outage probability (in presence of turbulence)
Direct Detection:		
Constant on for entire symbol	$\frac{2NN_I}{N_S^2} e^{-\left(\sqrt{N_S+\frac{N_S^2}{4}}-\frac{N_S}{2}\right)^2}$	$\frac{NN_I\theta_{thresh}}{N_S^2}\left(1+\frac{e^{4\sigma_\chi^2}-1}{N}\right)^3$
Constant on for half symbol	$\frac{NN_I}{4N_S}$	$\frac{NN_I}{2N_S}\left(1+\frac{e^{4\sigma_\chi^2}-1}{N}\right)$
Gaussian on for entire symbol	$\frac{NN_I}{2N_S} e^{-1/2}$	$\frac{NN_I}{2N_S}\sqrt{2\left(-\ln 2+\theta_{thresh}\right)}\left(1+\frac{e^{4\sigma_\chi^2}-1}{N}\right)$
Gaussian on for half symbol	$\frac{NN_I}{N_S} e^{-1/4}$	$\frac{NN_I}{2N_S}\left(2\sqrt{-\ln 2+\theta_{thresh}}+1\right)\left(1+\frac{e^{4\sigma_\chi^2}-1}{N}\right)$
Canceling on for entire symbol	$\frac{NN_I}{N_S}$	$\frac{2NN_I}{N_S}$
Canceling on for half symbol	$\frac{NN_I}{2N_S}$	$\frac{NN_I}{N_S}$
Homodyne Detection:		
Gaussian	$\frac{N_I}{4N_S} e^{-1}$	$\frac{N_I}{4N_S}\left(-\ln 2+\theta_{thresh}\right)\left(1+\frac{e^{4\sigma_\chi^2}-1}{N}\right)$
Canceling	$\frac{N_I}{4N_S}$	$\frac{N_I}{2N_S}\left(1+\frac{e^{4\sigma_\chi^2}-1}{N}\right)$

Table 2.2. Error probability and outage probability for various interferer types when the interferer uses the worst case duty cycle.

Figure 2.7 plots, for an atmospheric turbulent channel, the worst case interferer duty cycle and the corresponding outage probability for the various interferer types when the error probability threshold is 0.1. The interferer can cause worse performance if we use direct detection than if we use coherent detection. For homodyne detection, the canceling interferer causes the worst (highest) outage probability because none of this interferer's energy is wasted. For direct detection, Gaussian interference that is on for half the symbol is the most damaging for large error probability thresholds. Both tails of the Gaussian interferer cause outages.

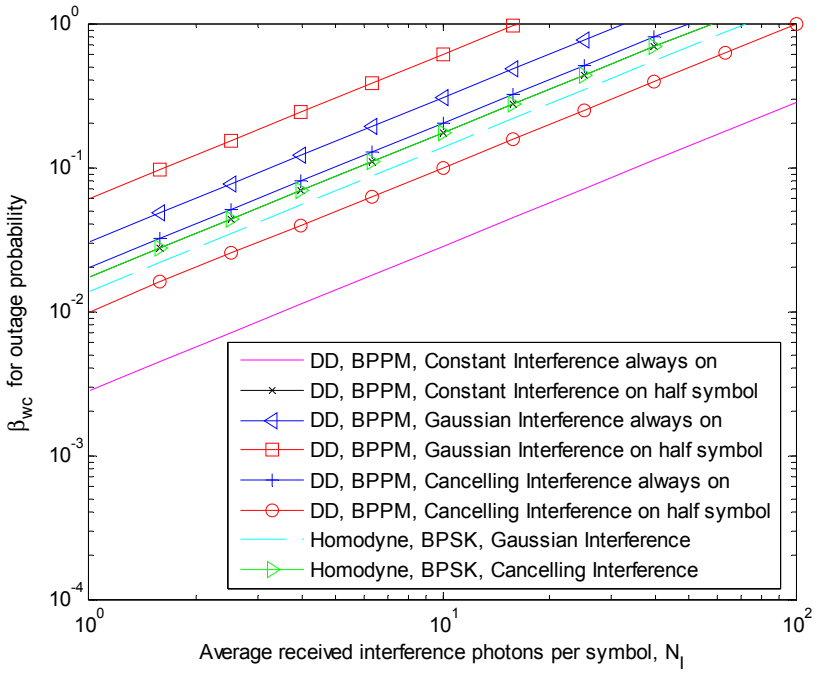

(a)

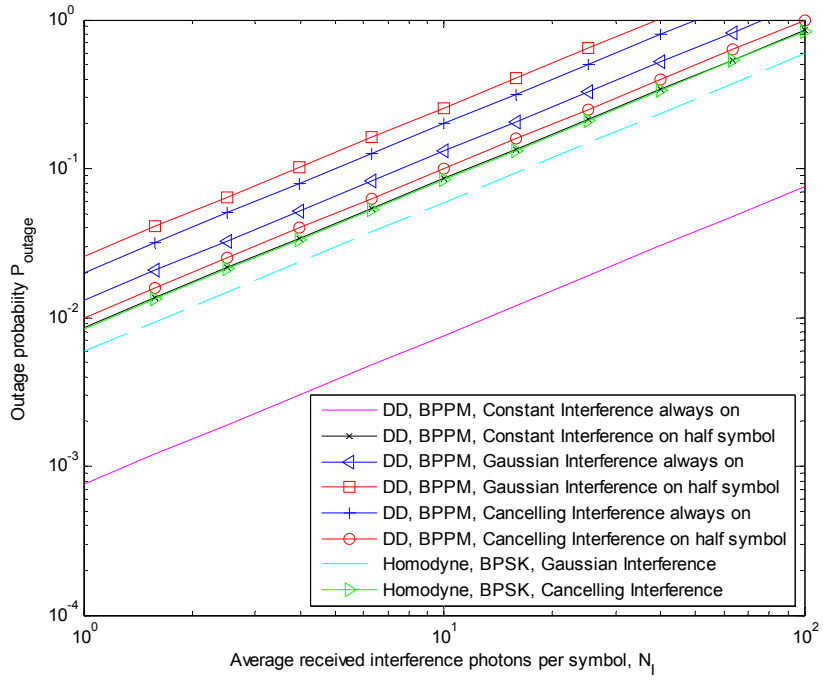

(b)

Figure 2.7. a) Interference worst case duty cycle b) outage probability of direct detection and homodyne detection in the presence of interference that uses the worst case duty cycle in the following conditions: log normal fading with σ_χ =0.3, P_e^{thresh} =0.1, N_S=100, N=1, N_n=1

Next we derived the power gain of diversity homodyne detection over diversity direct detection in the presence of and absence of the worst interferer (canceling interferer in coherent detection and Gaussian interferer that is on for half the symbol in direct detection). The results are summarized in Table 2.3.

Diversity in direct detection and homodyne detection	Power Gain of diversity homodyne detection over diversity direct detection
Presence of interferer	
Direct detection and homodyne detection use diversity N	$\left(2\sqrt{-\ln 2+\theta_{thresh}}+1\right)N$
Direct detection uses diversity N, homodyne detection uses diversity N_{opt}	$\frac{N_{opt}\left(2\sqrt{-\ln 2+\theta_{thresh}}+1\right)\left(1+\frac{e^{4\sigma_\chi^2}-1}{N_{opt}}\right)}{\left(1+\frac{e^{4\sigma_\chi^2}-1}{N}\right)}$
Direct detection uses diversity N, homodyne detection uses diversity $N_{optGaussianHalfSymbolInterference}$	$\frac{\left(2\sqrt{-\ln 2+\theta_{thresh}}+1\right)e^{4\sigma_\chi^2}}{\left(1+\frac{e^{4\sigma_\chi^2}-1}{N}\right)}$
Absence of Interferer	
Direct detection and homodyne detection use diversity N	$2\frac{\theta_{thresh}+\sqrt{2\theta_{thresh}NN_n}}{(1+N_n)(-\ln 2+\theta_{thresh})}$
Direct detection uses diversity N, homodyne detection uses diversity N_{opt}	$k_1\exp\left\{\begin{matrix}-\sqrt{-2\ln(2P_{outage})\ln\left(1+\frac{e^{4\sigma_\chi^2}-1}{N}\right)}\\ -\frac{1}{2}\ln\left(1+\frac{e^{4\sigma_\chi^2}-1}{N}\right)\end{matrix}\right\}$ where $k_1=2\left(\frac{\theta^{thresh}+\sqrt{2\theta^{thresh}N_{opt}N_n}}{(1+N_n)(-\ln 2+\theta^{thresh})}\right)\sqrt{1+\frac{e^{4\sigma_\chi^2}-1}{N_{opt}}}\cdot\exp\left\{\sqrt{-2\ln(2P_{outage})\ln\left(1+\frac{e^{4\sigma_\chi^2}-1}{N_{opt}}\right)}\right\}$
Direct detection uses diversity N, homodyne detection uses diversity $N_{optGaussianHalfSymbolInterference}$	$c_1\exp\left\{\begin{matrix}-\sqrt{-2\ln(2P_{outage})\ln\left(1+\frac{e^{4\sigma_\chi^2}-1}{N}\right)}\\ -\frac{1}{2}\ln\left(1+\frac{e^{4\sigma_\chi^2}-1}{N}\right)\end{matrix}\right\}$ where $c_1=2\left(\frac{\theta^{thresh}+\sqrt{2\theta^{thresh}N_n}}{(1+N_n)(-\ln 2+\theta^{thresh})}\right)e^{2\sigma_\chi^2}\exp\left\{\sqrt{-2\ln(2P_{outage})4\sigma_\chi^2}\right\}$

Table 2.3. Power gain of homodyne detection (in the presence of canceling interference) over direct detection (in presence of Gaussian interference that is on for half symbol)

Background noise in the receiver field of view couples into the receiving detection system. Direct detection systems are phase insensitive systems and each sub-aperture will admit one mode of background noise. Whereas in a coherent system, the received signals of the sub-apertures are coherently combined and thus only one spatial mode of background noise couples into the detection process. Figure 2.8 plots the power gain of diversity homodyne detection over diversity direct detection. In the *absence* of interference, when direct detection's diversity is increased blindly together with coherent detection's diversity, the power gain is proportional to the square root of the diversity, $\sqrt{N}$.. The reason for this gain is whereas coherent detection can track and coherently combine the fields from the individual apertures, incoherent detection does not and thus suffers incoherent combining loss. In the *presence* of an intelligent interferer, if direct detection's and coherent detection's diversity are increased together, the power gain actually increases proportional to the diversity *N* (even larger than in the absence of interference). This is due to the increase in unwanted interference detected by direct detection as diversity increases, together with the fact that the interferer duty cycle is worst case (and a function of the communication system including diversity).

Since direct detection's performance worsens if diversity is increased beyond an optimal value, and coherent detection's performance always improves with diversity, one may argue that a fairer comparison of the two systems occurs if direct detection's diversity is fixed to the optimal value (assuming an interferer is present or absent), and coherent detection's diversity is allowed to vary. This power gain approaches an asymptote because there is a limit to the amount of outage statistic improvement. We see, though, that the power gain is significant and that most of the benefit of diversity coherent detection can be achieved with a small amount of diversity. An added benefit of diversity coherent detection is that it does not result is worse performance if a large diversity is chosen (as in the case of diversity direct detection).

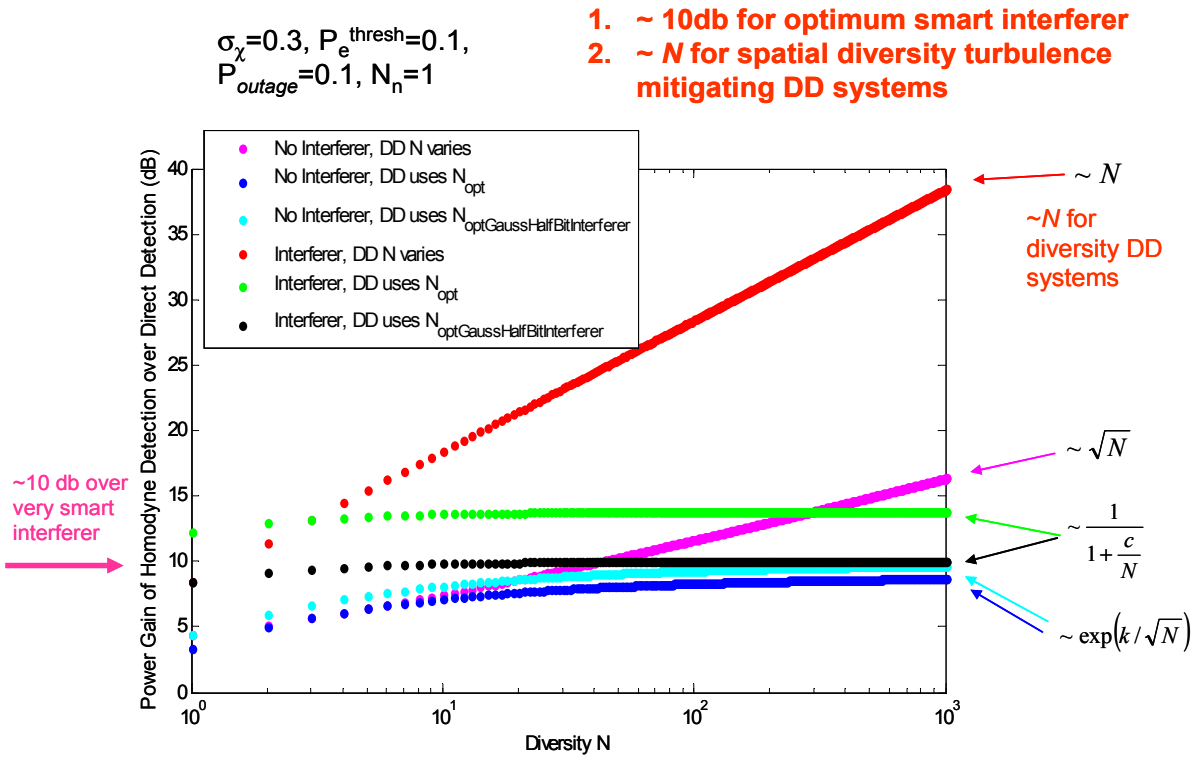

Figure 2.8. Power Gain of homodyne detection over direct detection (if interference is present and it uses the worst case duty cycle) for outage probability of 0.01 when σ_χ =0.3, P_e^{thresh} =0.1, N_n=1. N_{opt}=6.

2.4 Double balanced mixer for frequency spreading and de-spreading

Figure 9 shows one of many realizations of a double balanced mixer coherent receiver. It is used to take out transmitter band-spreading with an LO laser band-spread by the same key via nonlinear mixing after optical detection, as shown in Figure 2.9. This previous experiment was done with a communication rate of 1 Mbps and a band-spread of 1 GHz.

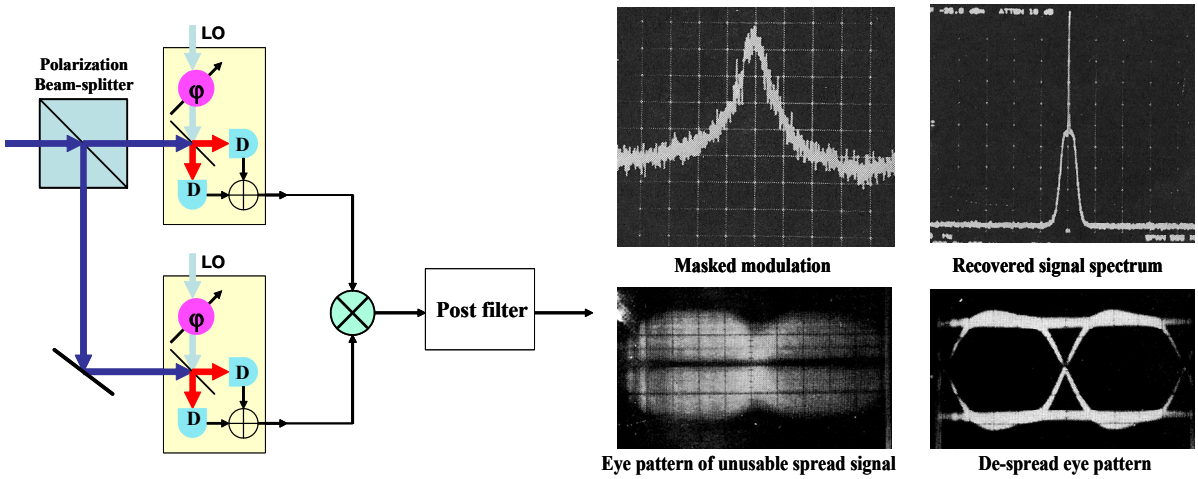

Figure 2.9. Double balanced mixer coherent receiver for de-spreading of crypto-key driven frequency spread transmission for low LPI. The data rate is 1Mbps with 1 GHz spreading.

2.5 Spatial mode modulation for near-field anti-jam (AJ) and multiple-access communication.

If the receiver is in the near-field of the transmitter, it is possible to modulate the received spatial mode of the signal and via feedback to the transmitter select a spatial mode with as small an overlap (small inner product) with the interfering field as possible. An idealized example is given in Figure 2.10, where the received signal field is manipulated via transmitter control into the 01 mode, with the two lobes having opposite phase and is thus orthogonal to a jamming field in a 00 mode. In a time scale faster than 1 mS, the turbulence can be considered frozen and the transmitter with the aid of receiver feedback selects amplitudes and phases of each element so that the received field ψ and the jamming field ξ have inner products $\left|\langle \xi, \psi \rangle\right|^2 \sim 0$

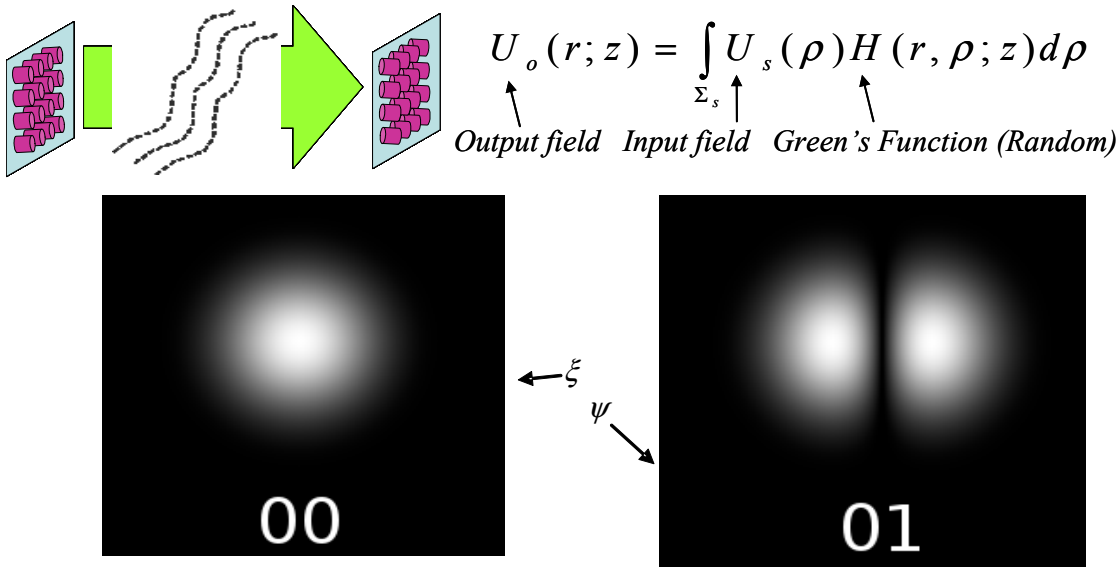

Figure 2.10. Spatial mode modulation for near-field AJ and multiple-access communication.

3 Heterogeneous Defense Network Study

Sponsors
DARPA – Future Defense Network Study: HR0011-08-1-0008

Project Staff and other Participants
Vincent W. S. Chan, John Chapin (MIT and Vanu Inc), Anurupa Ganguly, Lillian Dai, Paul Lencioni (Cisco Systems), Greg Ackers (Cisco Systems), Ori Gerstel (Cisco Systems), Eric Swanson, Guy Weichenberg, Vince Poor (Princeton), Renaldo Vellenzveula (Bell Labs.), Bob Brodersen (UC Berkeley), Ada Poon (Stanford University), Balaji Prapbakar (Stanford University), Namish Patel (Sycamore Networks)

The primary goal of a defense network should be: To enable users to obtain and share necessary and timely information in the right form over an integrated heterogeneous dynamic network which is scalable and evolvable, Figure 3.1**.** The performance metric most important to the end users is the ability to get the end products they need in a timely fashion with integrity. How it is being done technically is secondary. The data must be in usable form within the constraints of the network such as bandwidth, delays and display capabilities and resolution. The network must be a single integrated and also heterogeneous network so users connected to different communication modalities can communicate with each other. This integration spans from the Physical Layer to all higher Layers of the protocol stack of the network and must accommodate the reality of the heterogeneity of communication modalities and capacity constraints. Many of the tough network problems at or near the network edge are yet to be fully solved and it should be a first priority to address these problems immediately before they impact large acquisition programs. The architecture research study is designed to uncover though networking problems especially those tied to physical layer communication system properties and explore architecture constructs that may provide realistic solutions for the realization of an integrated heterogeneous defense network.

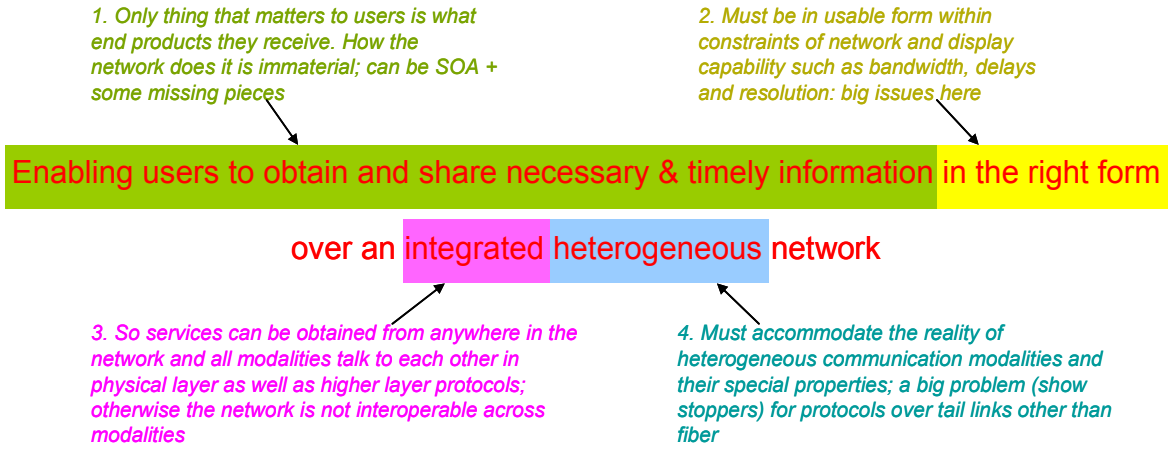

Figure 3.1Integrated heterogeneous defense network.

The following is a set of high level architecture goals of an integrated heterogeneous defense network and we will use them to guide our research (all of these, except for 3, are innovative architecture ideas that will be developed in this study):

1. The Defense Network should be heterogeneous and accommodate multiple types of networks of different generations with the integration into a single interoperable network via gateways between disparate subnets and a Master Control Plane for subnet integration.

2. The Defense Network should have the following two-tiered network services, Figure 3.2:

a. *A robust MINIMUM "hard-core" network service necessary for successful defense operations. This service will have modest rates but solid connectivity at all times with low delays and designed and tested to be bullet proof.*

b. *A much higher rate "soft-shell" network, which is less robust but higher rates and support high rate services such as web-based Service Oriented Architectures.*

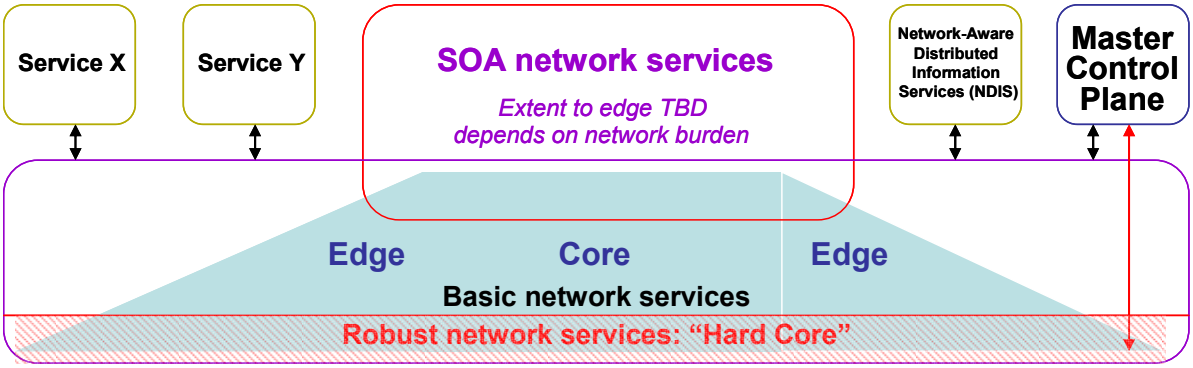

Figure 3.2 Defense network architecture with two-tiered robust "hard-core" network services (for time critical and network management control messages) and basic network services

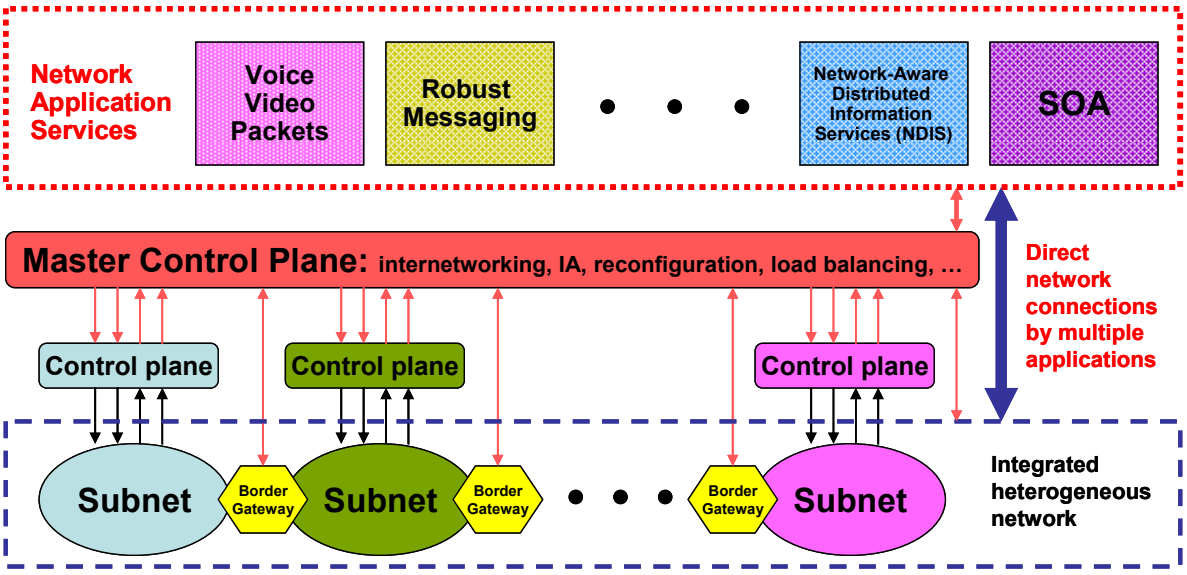

Figure 3.3 Integrated heterogeneous defense network with voice, video, data, hybrid IP and circuit based services.

3. The integrated network should support voice, video, data, hybrid IP and circuit based services.

4. There are critical outstanding architecture and technology issues of infrastructure-less wireless networks and some SATCOM networks, Figure 3.

5. It is important to examine the new concept of a Master Control Plane to facilitate internetworking and Information Assurance: critical for the integration across subnets/domains, interoperability, priority/policy enforcement, access control and security, Figure 3.3.

6. The proliferation of information and data services to the tactical edge will generate and consume vastly more bandwidth in the future and will saturate the backhaul network. A Network-aware Distributed Information Service (NDIS) should be deployed near the network edges to adjust user behavior as the network changes to maintain critical services on the network, Figure 3.3.

This study will continue in the next year and a strawman architecture will be constructed.